Novel Bridge over Water Detection Algorithm from LiDAR Data Based on Skinny Triangle

Yansong Zhao, Su Lv, Yanling Li and Xuelin Zhao

Abstract—**It is significant to detect the bridge from LiDAR automatically and quickly, which is regarded as an important artificial building and transport hub. In this paper, a skinny triangle-based detection algorithm of bridge over water is proposed. First, Triangulated Irregular Network(TIN) is generated in LiDAR data, during which a skinny triangle is used to detect points on the river edge and bridge, and the elevation difference between them is used to separate those points. Second, a nonlinear classifier designed with TIN is used to separate the LiDAR points on the river edge. Points of bridge borders can be separated automatically and adaptively according to the collinear characteristics of the bridge border. Finally, creating fitted curves to obtain river bank and bridges borders respectively. The coordinate of bridge angular points can be obtained by solving the equations set, which is consists of the river bank curve and bridges borders curve simultaneous. The experimental results demonstrate that the proposed algorithm can perform well to extract bridge over water from LiDAR data.**

Index Terms—**LiDAR data, TIN, skinny triangle, edge points separated, curve fitting**

I. Introduction

WITH the rapid development of 3D laser scanning technology, point cloud data with a series of features can be acquired directly and quickly by laser scanner. In civil construction, laser scanning technology is also widely used, and the obtained data will be used for 3D modeling. In this paper, bridge extraction research is carried out based on point cloud data scanned at civil construction sites. The data has the characteristics of wide range, large amount of data and irregular distribution of non-target point cloud. Therefore, it is necessary to use appropriate filtering algorithm to filter the non-target points with different color, shape and scope[1]. Airborne LiDAR can directly obtain three dimensional geography information, the advantages of which are large-scale, high-precision, high-efficiency and low-cost, and it can do much better in constructing three dimensional city model than traditional photogrammetric methods do. The product of airborne LiDAR is a dense cloud of 3D points[2]. The points in the cloud are samples from the surfaces of the buildings, vegetations, bridges, rivers and other objects. Therefore, how to accurately detect the objects in it is pretty important[3], [4], [5], [6], [7], [8], [9]. Bridges, regarded as a kind of important artificial buildings and transport hubs, have induced great attention by the military, commercial and civilian users[10], [11]. Bridge object detection from LiDAR data is of great significance. Many bridge detection approaches have been proposed in computer vision, remote sensing, and photogrammetr[12], [13], [14]. Trias-Sanz et al. proposed an approach to detect bridges in high resolution satellite imagery[15]. The procedure starts from segmenting an image and then classifies the generated segments with a neural network. Then, rules are defined to classify segments as bridge or other class. Houzelle et al. suggested a data fusion technique for SPOT and SAR images to detect bridges and extract urban area[16], [17]. For bridge detection, they first separate water in the SPOT image to spatially constrain the location of bridges in the SAR image. Mandal et al. used the method of analyzing the IRS satellite imagery to detecting various man-made objects including bridges[18]. Initially, a multi-valued recognition system is used to classify the image pixels into six land-cover types. In order to identify the targets, knowledge of their characteristics and their interrelationship is incorporated into the clustered image using heuristic rules. D. Chaudhuri et al. presented an approach to detect bridges over water bodies from multispectral image[19], [20]. The multispectral image is first classified into eight land-cover types using a majority-must-be-granted logic based on the multi-seed supervised classification method. Bridges are then recognized in this tri-level image by a knowledge-based approach which exploits the spatial arrangement of bridges and their surroundings with a five-step approach.

Generally, the bridge detection algorithm is mostly based on the aerial images[21], [22], [23], [24], [25], while the detection algorithm based on LiDAR data is scarcely ever found. Sithole et al. proposed an algorithm based on the analysis of profile to extract the bridge point[26], but for the bridge over water, it has a lower efficiency because the water body should be detected previously. Li et al. presented a method which is capable to detect bridge over water or land bridge efficiently[27]. Unfortunately, the frequency use of Triangulated Irregular Network(TIN) location, insert and delete operation has a great effect on the efficiency of detection. Quite a few parameters in Li's algorithm also bring about the problem of parameter settings. A algorithm was proposed based on morphological filter and skeleton extraction in LiDAR data[28]. The more prior knowledge should be used and the LiDAR data should be transformed into grayscale image have an effect on the efficiency of the algorithm. A blank area exists if there is a water body

Manuscript received March 30, 2022; revised September 28, 2022.

This work was supported by National Natural Science Foundation of China (No. 31872704), Science and Technology Department of Henan Province (No.222102210265), and by Foundation of Henan Educational Committee under Contract (No.22A520007)

Yansong Zhao is an Associate Professor at the School of Foreign Language, Xinyang Normal University, Xinyang Henan, 46400, China. (e-mail: yansongxn@163.com).

Su Lv is an Associate Professor at the Information and Blockchain Technology, Xinyang Vocational College of Art, Xinyang Henan, 464000, China. (e-mail: stzwww@163.com).

Yanling Li is a Professor at the Computer and Information Technology, Xinyang Normal University, Xinyang Henan, 46400, China. (e-mail: lyl75@163.com).

*Corresponding author: Xuelin Zhao is an Associate Professor at the Computer and Information Technology, Xinyang Normal University, Xinyang Henan, 46400, China. (e-mail: xlz_cit@xynu.edu.cn).

because the laser spots are absorbed by the water. There are many skinny triangles of the water area in TIN when the LiDAR data is Delaunay Triangulated. This paper provides a new algorithm to detect the bridges over water from LiDAR data based on skinny triangle.

The rest of the paper is organized as follows. The detailed description of skinny triangle, the river and edge of bridges detection algorithm are given in Section 2. Section 3 presents our proposed method of bridge over water detection in detail. The experiments and results analysis are given in section 4. Finally, we conclude the paper in section 5.

II. The river and edge of bridges detection

A. Skinny triangle

Triangulated Irregular Network is a continuous triangle plane which is generated utilizing Delaunay triangulation on irregular distribution of discrete data points. A digital model or 3D representation of a terrain's surface using continuous irregular triangle surface, which is called Digital Surface Model(DSM)[29], [30], [31], [32], [33]. Due to the water characteristic of absorption of laser , which leads to the sparsity even disappearance of laser spot on water, a blank area will appear if there is water. When TIN is generated, the points in different sides of the river will constitute some triangles so that it is longer and narrower compared with the triangles of which three vertices are in the same side of the blank areas. Skinny triangle in trigonometry is a triangle whose height is much greater than its base. Applications of the skinny triangle occur in any situation where the distance to a far object is to be determined. This can occur in surveying, astronomy, and also has military applications. There will be some skinny triangles in TIN when the LiDAR data is Delaunay Triangulated[34], [35]. As shown in Fig.1, we can determine whether the triangle is across the river or not based on the type of a triangle in TIN.

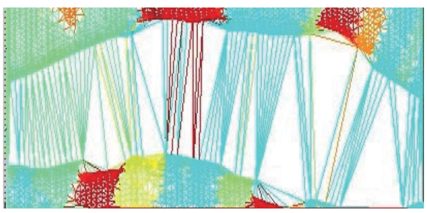

Fig. 1. Triangles across blank area

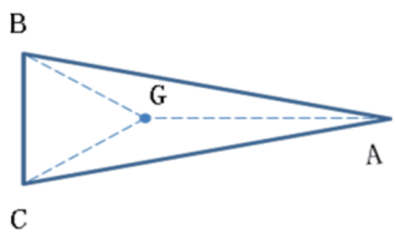

Fig. 2. Skinny triangle

B. Judgement of skinny triangle

The key to detect the river edge points with skinny triangle is how to determine the triangle is a skinny triangle. In this paper, we define a quantitative calculation formula for Skinny Degree as follow.

Definition 1: Skinny Degree(δ_{SD}) is the quadratic sum of the distance from each vertice of the three vertices to the barycenter. For the i^{th} triangle, its Skinny Degree(δ_{SD}^{i}) is calculated by equation(1).

$$\delta_{SD}^{i} = |A_iB_i|^2 + |A_iC_i|^2 + |B_iC_i|^2 \tag{1}$$

Where A_i, B_i, C_i are the three vertices and G_i is the barycenter of the $i^{th}, i = 1, 2, \cdots, N$ triangle, N denotes the number of the triangle in TIN. If δ_{SD}^{i} satisfies the inequality $\delta_{SD}^{i} > threshold$, we regard the i^{th} triangle as a skinny triangle.

It is not in a three-dimensional space, but in the plane when calculating Skinny Degree and judging the skinny triangle, only the x and y-coordinate of the three vertices and barycenter used. In fact, we assume that z-coordinate is set to 0 when calculating. It is considered to be a skinny triangle as long as the calculated result is greater than the threshold of skinny triangle. Therefore, it will be calculated correctly, and it has nothing to do with attribute (such as equilateral, isosceles, ordinary) of spatial triangle.

C. The threshold settings and edge points selection

Because the three vertices of non-skinny triangle are very close to each other, of which the arbitrary distance is approximately equal to the precision of LiDAR system, and the Skinny Degree of the non-skinny triangle is smaller. Because of the fact that the three vertices of the skinny triangle are in the different sides of the blank area and the width of river is considerable larger than the precision of LiDAR system, the Skinny Degree of the skinny triangle is very large. As a consequence, appropriate larger threshold of Skinny Degree should be selected.

The threshold should be set associated with the accuracy of the LiDAR system by which the LiDAR data is obtained. As the triangle shown in Fig.2, G is the barycenter of $\triangle ABC$, the in-equation(2) is established.

$$|AG|^2 + |AG|^2 + |BG|^2 < |AB|^2 + |AC|^2 + |BC|^2 \tag{2}$$

Generally, for the non-skinny triangle, $|AB|^2 < \varepsilon^2$(ε is the accuracy of the LiDAR system), $|AC|^2 < \varepsilon^2$, $|BC|^2 < \varepsilon^2$. So the in-equation(3) is obtained.

$$|AG|^2 + |AG|^2 + |BG|^2 < |AB|^2 + |AC|^2 + |BC|^2 \leq 3\varepsilon^2. \tag{3}$$

According to in-equation(3), the threshold of skinny triangle is determined, and $3\varepsilon^2$ is appropriate. Due to the deviation of the system, the threshold should be greater than $3\varepsilon^2$.

Skinny triangle will not be got until the Skinny Degree of triangles are all calculated in TIN. The three vertices of a skinny triangle should be selected as the edge points, As is shown in Fig.3 and Fig.4. Fig.3 is the original LiDAR data and the Fig.4 is the edge points being selected with our method.

III. Detection of bridge over water

A. Separation of the river edge and bridge border

To deal with points of the river edge and points of bridges borders effectively, the points of the river and points of the

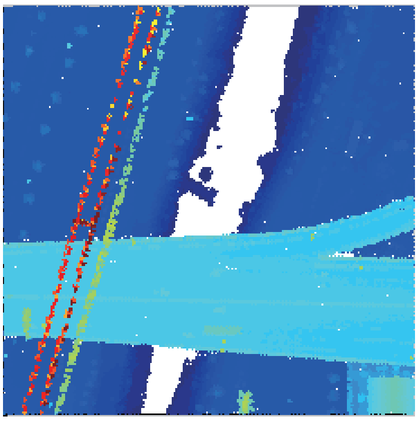

Fig. 3. Original LiDAR data.

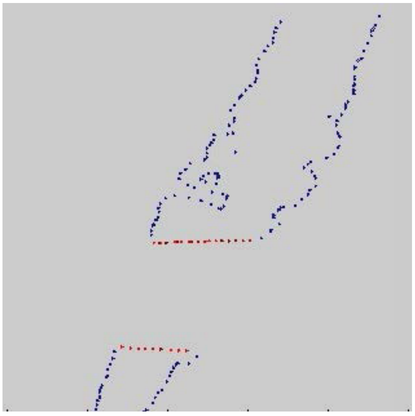

Fig. 4. Edge points selected.

bridges borders should be separated. Generally speaking, the height of river points is much smaller than the height of bridge points, and the height of river and bridge points vary continuously. If the elevations of all the edge points are sorted in ascending order, we can get the result shown in Fig.5. Similarly result can be obtained as the result in Fig.5. Intuitively, the conclusions can be obtained as follows: the left part of the point A is the curve of elevation change of river edge points, and the right part of the point B is the curve of elevation change of bridge borders points. Point A and B are the boundary points of the curve that the points' elevation varies of the river edge and bridge border. Obviously, significant changes of elevation emerge between point A and point B. Thus we can separate the river edge points and borders edge points according to the characteristics mentioned above. Given a certain threshold, the point whose elevation is greater than the threshold is marked as a point of bridge border, otherwise it is regarded as a point of river edge. The key to separate the points of river edge and the points of bridge border is how to find a appropriate elevation threshold. If $H(A)$ is regarded as the elevation threshold, some the points of river edge will be regarded as the points of bridge border incorrectly. Similarly, if $H(B)$ is regarded as the elevation threshold, some points of the bridge border will be divided into the points of river edge incorrectly. To reduce the possibility of misclassification and improve the accuracy of classification, a weighted average method is adopted to obtain elevation threshold $H_{thresdhold}$

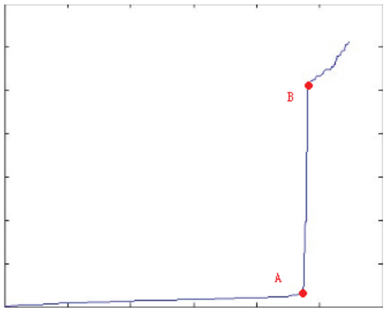

Fig. 5. The elevation changes of edge point

in this paper. The $H_{thresdhold}$ is calculated by equation(4).

$$H_{thresdhold} = \alpha H(A) + \beta H(B). \quad (4)$$

Where $\alpha + \beta = 1$ and $H(x)$ is the elevation of point $x, x \in A, B$. Because $H(A)$ and $H(B)$ satisfy the in-equation $H(A) < H(B)$, the in-equation(5) is obtained.

$$H(A) < \alpha H(A) + \beta H(B) < H(B). \quad (5)$$

In our work, a lot of experiments are conducted. The best value of α and β are will be set to 0.45 and 0.55 respectively with the purpose of minimizing the possibility of misclassification.

From Fig.5, we can see that great changes of elevation happen at the point A, causing a large gradient of point A. The gradient can be used to calculate the elevation of point A and B by equation(6)-(9).

$$\bigtriangledown H(P(k)) = H(P(k+1)) - H(P(k)), k = 1, 2, \cdots, N, \quad (6)$$

$$k_{best} = arg\max_{k} (\bigtriangledown H(P(k))) \quad (7)$$

$$H(A) = H(P(k_{best})) \quad (8)$$

$$H(B) = H(P(k_{best} + 1)) \quad (9)$$

where P is a vector which stores the elevation of the points of river edge and bridge border with ascending order. N is the number of the points in P. The result of the separation is shown in Fig.6, in which red represents the points of bridge border, while blue stars denote points of the river edge.

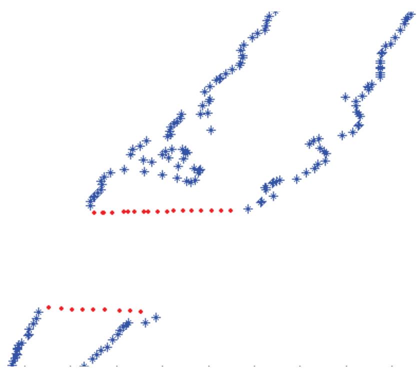

Fig. 6. Edge points separated (Sample data)

B. Separation of river edge points

After separating the points of river edge and the points of bridge border, we need to deal with the points of river edge and the points of bridge border to utilize the two banks of the river and to obtain two fitted curves respectively due to that two banks of a river are unparallel and cannot overlap each other by translations. River edge points in the plane is separable, so a curve can be found to divide two bank of the river edge points into two parts and each of them belongs to a river bank. In this paper, the edge points of the river are projected onto a plane. We can get the curve with TIN according to the following procedure.

$$G = \{(x_{G_i}, y_{G_i}), \delta^i_{SD} > thresd\} \qquad (10)$$

Where (x_{G_i}, y_{G_i}) is the barycenter and A_i, B_i, C_i are the three vertices of $\triangle A_iB_iC_i$ The constant $thresd$ is the threshold of skinny triangle. A fitted curve $RG(x, y) = 0$ will be gained by doing curve fitting the point with the G. We can separate the two banks with classifier $RG(x, y) = 0$.

With a classifier, we can set up the criteria of classification, and regard (x_i, y_i) as the point of the first bank if (x_i, y_i) satisfies the inequality $RG(x_i, y_i) > 0$. We regard (x_i, y_i) as the point of second bank if (x_i, y_i) satisfies the inequality $RG(x_i, y_i) < 0$. As a result, the separation of the river edge points is completed. The edge points of two banks can be separated into two parts successfully in this way. For the Sample data, the result of separation is shown in Fig.7. Red dots and blue dots denote different bank of the river respectively.

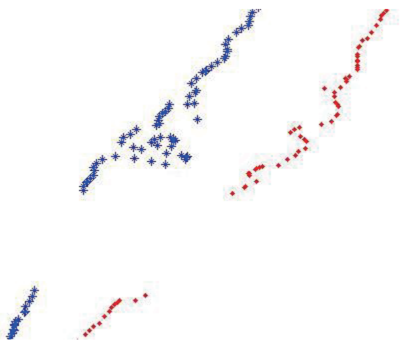

Fig. 7. River edge points separated (Sample data)

C. Separation of the points of bridge edge

To obtain the fitted curve of each border of the bridges, it is necessary to separate edge points of all the bridges which means to store different border points of each bridge separately. In this paper, we assume that the border of bridge is a straight line or almost a straight line. Thus, it will form a line when curve fitting is adapted after the bridge edge points being projected onto the horizontal plane. The distance from all points at the same border is small even almost to zero. According to this fact, the LiDAR points on the different border of a bridge and different bridges can be separated. The separation algorithm(1) is presented as follows.

Where U is the set which is storing the points of bridge border separated. Because the bridge border is a straight or almost a straight line, a small threshold value of should be given. When the algorithm stopped, $k/2$ is the number

Algorithm 1: The algorithm of separation of the points of bridge edge.

Input: border points of bridge B, the threshold of distance σ;
Output: the result of separation U;
Initialization:$U = \{\}$, $k = 1$;
while $B \neq \{\}$ **do**
  Put all the points of bridge border in set B in ascending order;
  Pick up the first three points from and fitting them to a straight line $L_k(x, y) = 0$, set $i = 1$;
  Calculate the distance d from the point (x_i, y_i) to the line $L_k(x, y) = 0$;
  if d *satisfies the in-equality* $d < \sigma$ **then**
    $U(K) = U(k) \cup (x_i, y_i)$;
    $i = i + 1$;
  else
    $B = B - U(k)$;
    $i = 1, k = k + 1$;
  end
end

of bridges, and the coordinates of bridge border points are stored in U. Besides, in the algorithm(1), the points of bridge border need to be sorted in ascending order, so we have to determine which coordinate should be used. we put forward a method for selecting the coordinate as equation(11).

$$|B(1) - B(2)| < \gamma \qquad (11)$$

Where γ is the distance threshold between point $B(1)$ and $B(2)$. Generally, a very small value is chosen, such as 1 is used in this paper. When sorting according to the y-coordinate, we need to sort the set B according to the x-coordinate if the in-equality(11) is not satisfied.

D. The determine of angular point of bridge

While the points of river and bridge border LiDAR are separated, it is easy to obtain curve equations of the bank of river and borders of bridges by fitted curve. After that, curve equations of the bank of rivers and the borders of bridges are combined into a equations set, as shown in equation(12). Coordinates of bridge angular points can be obtained by solving the equations.

$$\begin{cases} RL_i(x, y) = 0 & i = 1, 2. \\ BL_j(x, y) = 0 & j = 1, 2, \cdots, m \end{cases} \qquad (12)$$

Where $RL_i(x, y) = 0, i = 1, 2.$ is the curve equations that the bank of a river and the curve equations $BL_j(x, y) = 0, j = 1, 2, \cdots, m$ is fitted by the edge points of j^{th} bridge. m is the number of bridges.

Assuming that the length of a river is considerable large, if we fitting the bank of river into one curve as before, it may affect the accuracy of coordinates of the angular point, even cause some errors. we segment the river bank to several sections according to the number of bridges on the river by a linear classifier to classify the river edge points with the help of the fitted curve we have done before. To improve the accuracy of the angular points of bridges, the strategy of the river segmentation will be used. For the sake of achieving segment the bank of the river, bridge border curve equations can be regarded as a linear classifier. This step can eliminate errors caused in the process of fitting curve, as well to improve the accuracy of angular points of the river. After that, curve equations of the bank of river and borders of bridge are combined into an equations set, as shown in equation(13).

$$\begin{cases} RL_i k(x,y) = 0 & i = 1,2; k = 1,2,\cdots \\ BL_j(x,y) = 0 & j = 1,2,\cdots,m \end{cases} \tag{13}$$

Where $RL_i k(x,y) = 0$ is the curve equation which is k^{th} segment of the i^{th} bank of a river. $BL_j(x,y) = 0, j = 1,2,\cdots,m$ has the same meaning as in equation(12). By solving the equation set and obtaining the coordinate of angular point of each bridge, all bridges in LiDAR data can be detected and marked.

E. The detection algorithm of bridge over water

We need to delete some improper edge points to avoid the extraction of wrong edge points because the data of some singular points may bring some errors in edge detection. Then the TIN is established with the LiDAR data to calculate δ_{SD} of each triangle, marking the skinny triangles if δ_{SD} is larger than threshold. Finally, checking the skinny triangles to get the points of river edge and bridge border respectively. In addition, solving the equations to get coordinate of angular points. Fig.8 gives a flow chart of the whole process.

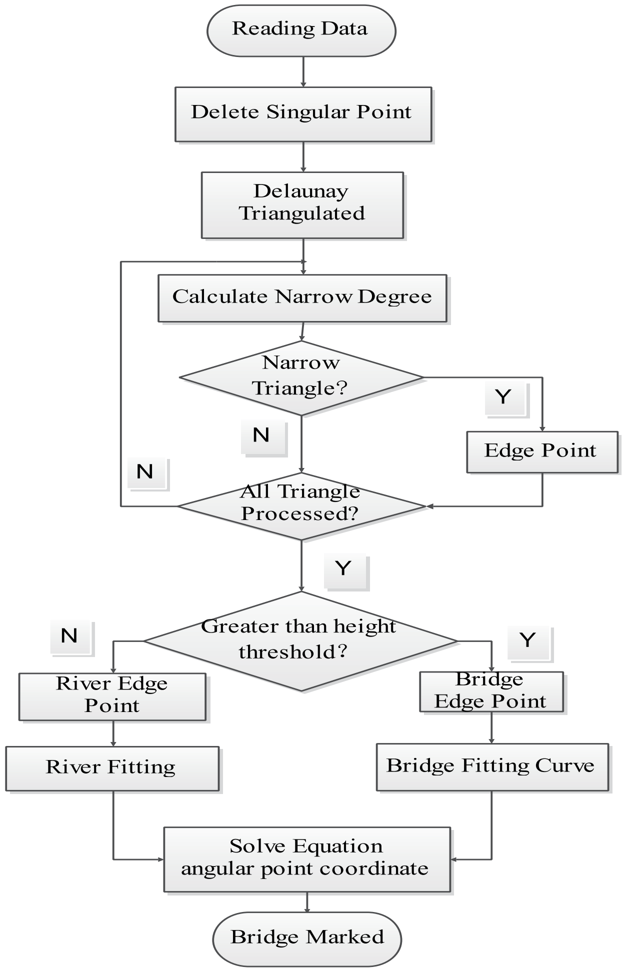

Fig. 8. Flow chart of bridge detection algorithm

IV. Experiments and analysis

A. Experimental results

The experiments are done on two other datasets. Sample dataset A has 52,198 points, two bridges. Sample dataset B has 218,134 points, three bridges. Each step of the experimental result of bridges detection is given respectively for empirical dataset in Fig.9 and Fig.10. Fig.9(a) and Fig.10(a) are the original data of LiDAR data, and the color of the points in LiDAR data rendering according to the elevation. Fig.9(b) and Fig.10(b) are the results of Delaunay Triangulated on the original data. Fig.9(c) and Fig.10(c) are the points of river and bridge edge detected. In Fig.9(d) and Fig.10(d), the red area denotes the bridges detected. Form the subfigure(d), we know that all the bridges in sample dataset A and B have been detected correctly. In this paper, the constant 100 is regarded as the threshold of Skinny Degree. Distance threshold that from point to the line $\sigma = 1.5$ and distance threshold $\gamma = 1$ are selected.

We also compare our bridge recognition method with the other methods in literature[14], [26], [28]. From the result in Fig.11(a), we can see that only one bridge is detected. The reason is that the surroundings of the bridges are complicated. In Fig.11(b), the heights of the bridges and the ground are similar, so two bridges are detected by Sithole G.'s algorithm. In Fig.11(c), three bridges are detected, but there are more prior knowledge should be used in the algorithm. In Fig.11(d), three bridges are detected by our algorithm and the prior knowledge doesn't needed. The constraint conditions are less and it is adaptable to a variety of bridges.

B. Analysis of experimental results

A large number of experiments are carried out in our experiments. The experimental results show that our algorithm can extract edge points of river and bridges effectively using the skinny triangle. Elevation information is used to separate the points of river edge and the points of bridge border adaptively. In the end, bridge angular points coordinate are calculated and bridges are detected, achieving the goal of accurate positioning for bridges over water in order to keep a high efficiency. Some parameters need to be set up, but it is simple. So the algorithm is available and efficient.

V. Conclusion

This paper proposes an algorithm for bridge detection over water. In this algorithm, the characteristic of the TIN with a river area is analyzed and a quantitative calculation formula of the Skinny Degree of a triangle is given. Then, the river and bridge edges points are obtained. The river edge points and bridge border points are separated using the elevation information. A classifier is designed to divide the bank of the river into two parts. It is adaptive to separate the points of bridge border using the bridge border almost a straight line. After that, curve equations of the bank of river and border of bridge are combined into an equation set. Bridge angular points coordinates can be obtained by solving the equation set. The experimental results show that the algorithm can

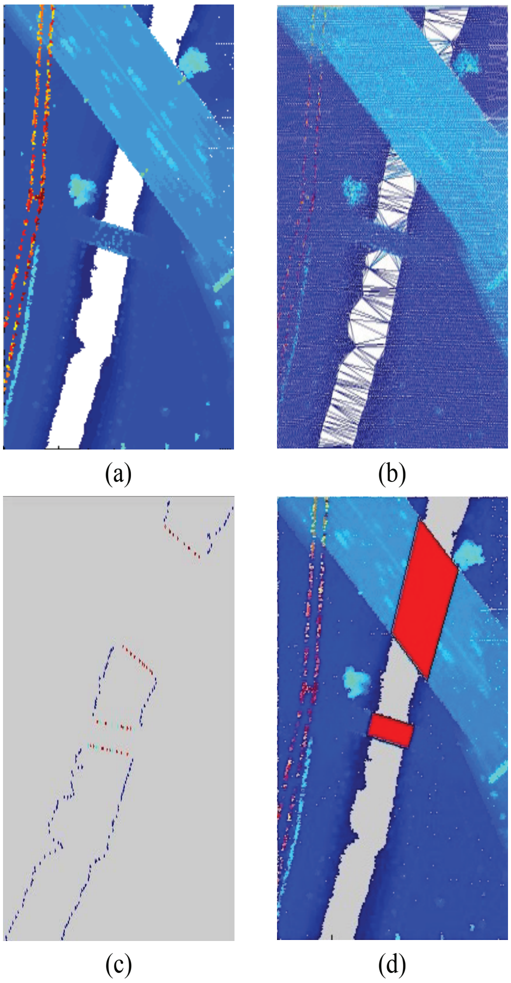

Fig. 9. Sample data A experimental results. (a)Original data; (b)Delaunay Triangulated; (c)Edge points detected; (d)Bridges marked.

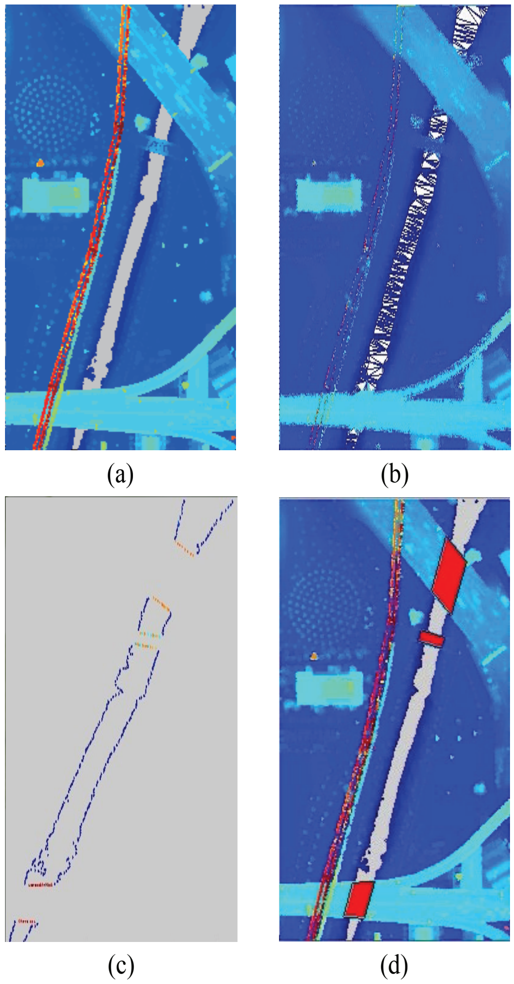

Fig. 10. Sample data B experimental results. (a)Original data; (b)Delaunay Triangulated; (c)Edge points detected; (d)Bridges marked.

accurately detect bridges over water and meanwhile maintain a high efficiency. However, the proposed method still has several flaws on which we need to do more research later. For instance, if the bridge and the bank of the river have an elevation almost approximately equal, how to separate the river edge points and bridges edge point efficiently remains an important problem.

REFERENCES

[1] J. K. YongSang Ryu, YoungSoo Park and S. Lee, "Image edge detection using fuzzy c-means and three directions image shift method," *IAENG International Journal of Computer Science*, vol. 45, no. 1, pp. 1–6, 2018.

[2] J. Liu and W. Wu, "Automatic image annotation using improved wasserstein generative adversarial networks," *IAENG International Journal of Computer Science*, vol. 48, no. 3, pp. 507–513, 2021.

[3] A. Rvid, V. Remeli, and Z. Szalay, "Raw fusion of camera and sparse lidar for detecting distant objects," *Automatisierungstechnik*, vol. 68, no. 5, pp. 337–346, 2020.

[4] Z. Luo, M. Attari, S. Habibi, and M. V. Mohrenschildt, "Online multiple maneuvering vehicle tracking system based on multi-model smooth variable structure filter," *IEEE Transactions on Intelligent Transportation Systems*, vol. 21, no. 2, pp. 603–616, 2020.

[5] R. Yue, H. Xu, J. Wu, R. Sun, and C. Yuan, "remote sensing data registration with ground points for roadside lidar sensors," *Remote Sensing*, vol. 11, no. 11, p. 1354, 2019.

[6] Z. Lingli, H. J, and K. A., "Photorealistic building reconstruction from mobile laser scanning data," *Remote Sensing.*, vol. 3, pp. 1406–1426, 2011.

[7] PengJ and L. YC, "Model and context-driven building extraction in dense urban aerial images," *International Journal of Remote Sensing.*, vol. 26, pp. 1289–1307, 2005.

[8] G. Raffaella, I. Antonio, and R. Daniele, "Height retrieval of isolated buildings from single high-resolution sar images," *IEEE Transaction on Geoscience and remote sensing.*, vol. 48, pp. 2967–2979, 2010.

[9] L. Taeyoon and K. Taejung, "Automatic building height extraction by volumetric shadow analysis of monoscopic imagery," *International Journal of Remote Sensing.*, vol. 34, pp. 5834–5850, 2013.

[10] W. Fan, W. Chao, Z. Hong, and Z. Bo., "Knowledge-based bridge recognition in high-resolution optical imagery," *Journal of Electronics Information Technology.*, vol. 28, pp. 587–591, 2006.

[11] S. G and V. G., "Automatic structure detection in a point-cloud of an urban landscape." *IEEE Workshop on Remote Sensing and Data Fusion over Urban Areas.*, vol. 2, pp. 67–71, 2003.

[12] C. Chao, Q. Qiming, and Z. Ning, "Extraction of bridges over water from high-resolution optical remote-sensing images based on mathematical morphology," *International Journal of Remote Sensing*, vol. 35, pp. 3664–3682, 2014.

[13] W. Baijian, L. Zhaoxia, and C. T. H. T., "Multiscale features and information extraction of online strain for long-span bridges," *Smart Structures and Systems.*, vol. 14, pp. 679–697, 2014.

[14] M. Qiguang, W. Wenqi, and X. Pengfei, "Novel algorithm for recognition of bridge in remote sensing image," *Acta Electronic Sinica.*, vol. 39, pp. 1698–1701, 2011.

[15] T.-S. R and L. N., *Automatic Bridge Detection in High-Resolution Satellite Images Computer Vision Systems.* New York: Springer Berlin Heidelberg, 2003.

[16] S.Houzelle and G.Giraudon., "Data fusion using spot and sar images for bridge and urban area extraction," *IEEE Geoscience and Remote Sensing Society.*, vol. 24, pp. 1455–1458, 1991.

[17] A. J. Santoso and Pranowo, "Medical image segmentation using phase-field method based on gpu parallel programming," *Engineering Letters*, vol. 30, no. 1, pp. 214–220, 2022.

[18] D.P.Mandal, C.A.Murthy, and S.K.Pal., "Analysis of irs imagery for detecting man-made objects with a multi-valued recognition system,"

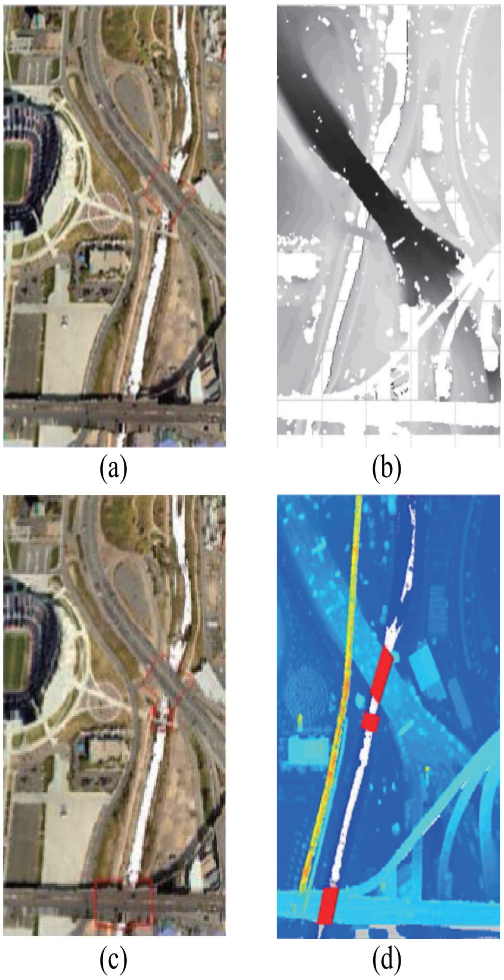

Fig. 11. Experimental results of sample data B. (a) Result obtained by method proposed in Ref[14]; (b) Result obtained by method proposed in Ref[26]; (c) Result obtained by method proposed in Ref[28]; (d) Result obtained by our algorithm.

IEEE Transaction on System, Man and Cybernetics., vol. 26, pp. 241–247, 1996.

[19] C. D and S. A., "An automatic bridge detection technique for multispectral images," *IEEE Transactions on Geoscience and Remote Sensing.*, vol. 46, pp. 2720–2727, 2008.

[20] Q. Zhou and S. Huang, "Strengthened change point detection model for weak mean difference data," *IAENG International Journal of Applied Mathematics*, vol. 50, no. 1, pp. 193–205, 2020.

[21] C. Chao, Q. Qiming, and C. Li., "Extration of bridge over water from high-resolution remote sensing images based on spectral characteristics of ground objects," *Spectroscopy and Spectral Analysis.*, vol. 33, pp. 718–722, 2013.

[22] Ma, Anderson, Crouch, and Shan, "Moving object detection and tracking with doppler lidar," *Remote Sensing*, vol. 11, no. 10, p. 1154, 2019.

[23] L. Jiancheng, M. Dongping, and S. Zhanfeng, "Research on bridge extraction from high resolution remote sensing image," *Application Research of Computer.*, vol. 23, pp. 151–153, 2006.

[24] C. Sheng, W. Hong, and S. Zhanfeng., "Study on object oriented extracting bridges from high resolution remote sensing image." *Journal of Images and Graphics.*, vol. 14, pp. 585–590, 2009.

[25] C. Xiangjun and G. Zhanfeng., "Data processing based on wavelet analysis in structure health monitoring system," *Journal of Computers.*, vol. 6, pp. 2686–2691, 2011.

[26] S. G and V. G., "Bridge detection in airborne laser scanner data," *ISPRS Journal of Photogrammetry and Remote sensing.*, vol. 61, pp. 33–46, 2006.

[27] L. Yunfan, M. Hongchao, and W. Jianwei., "Extracting bridges from airborne lidar data based on terrain features," *Geomatics and Information Science of Wuhan University.*, vol. 36, pp. 552–555, 2011.

[28] D. Yiping, S. Jianfeng, and M. Qiguang, "Bridge detection in light detecting and ranging data based on morphological filter and skeleton extraction," *Journal of Applied Remote Sensing.*, vol. 8, p. 083610, 2014.

[29] Z. Yi, W. Chengyi, and C. Jingbo., "A method of bridge outline extraction based on airborne lidar data." *Applied Mechanics and Materials.*, vol. 30, pp. 1048–1055, 2013.

[30] P. Y. Kong, "Computation and sensor offloading for cloud-based infrastructure-assisted autonomous vehicles," *IEEE Systems Journal*, vol. 14, no. 3, pp. 3360–3370, 2020.

[31] K. Deming, X. Lijun, and L. Xiaolu., "Equations of state calculations by fast computing machine," *IEEE Conference on Instrumentation and Measurement Technology.*, vol. 12, pp. 377–380, 2013.

[32] S. Kaasalainen and T. Malkamki, "Potential of active multispectral lidar for detecting low reflectance targets," *Optics Express*, vol. 28, no. 2, pp. 1408–1416, 2020.

[33] C. Liang, Z. Wei, and H. Peng, "Building region derivation from lidar data using a reversed iterative mathematic morphological algorithm," *Optics Communications.*, vol. 28, pp. 244–250, 2012.

[34] Z. Yongjun, W. Lei, and L. Liwen., "Automatic water body extraction based on lidar data and aerial images." *Geomatics and Information Science of Wuhan University.*, vol. 35, pp. 936–940, 2010.

[35] W. Zongyue, M. Hongchao, and X. Honggen., "A method for extracting water contour lines from lidar point clouds data." *Geomatics and Information Science of Wuhan University.*, vol. 35, pp. 432–435, 2010.